Cylindrical 2D ALE simulations of laser interactions with flyer targets

M. Kuchařík, J. Limpouch, R. Liska

Czech Technical University, Faculty of Nuclear Sciences and Physical Engineering, Břehová 7, 115 19 Prague 1, Czech Republic
e-mail: {kucharik, limpouch, liska}@siduri.fjfi.cvut.cz

Received 1 April 2006

We have developed 2D Arbitrary Lagrangian Eulerian (ALE) code in the cylindrical $r - z$ geometry. The ALE method overcomes problems with Lagrangian moving mesh distortion by mesh smoothing and conservative quantities remapping from Lagrangian mesh to smoothed one. The flyer target experiments [1, 2] performed at the Prague PALS laser facility are simulated by the developed code. The thin flyer disc is irradiated by intense laser beam and ablatively accelerated up to very high velocities (till 150 km/s) against a solid target. The high velocity impact of disc flyer on the target creates a crater. The high velocity impact simulations cannot be accomplished by standard Lagrangian code without the ALE method. The simulation results for several laser energies in 120-390 J range and laser basic and third harmonics compare reasonably with experimental data which include disc flyer impact velocities and crates sizes.

PACS: 52.65.Kj, 47.11.-j
Key words: plasma hydrodynamics, ALE, high-velocity impact, cylindrical geometry

1 Introduction

Laser plasma is typically modeled as a compressible fluid by Euler equations in Lagrangian coordinates. The Lagrangian approach with a computational mesh moving with the fluid suits better for compression and expansion regimes with moving boundaries, which appear regularly in laser plasma, than the Eulerian approach on the static mesh. Lagrangian hydrodynamical system with heat conductivity and laser absorption is given by

$$\frac{1}{\rho}\frac{d\rho}{dt} = -\nabla\cdot\vec{v}, \qquad \rho\frac{d\vec{v}}{dt} = -\nabla\cdot p, \qquad \rho\frac{de}{dt} = -p\,\nabla\cdot\vec{v} + \nabla\cdot(\kappa\nabla T) - \nabla\cdot\vec{I},$$

where t is time, ρ mass density, $\vec{v}$ speed, p pressure, e specific internal energy, T temperature, κ heat conductivity coefficient and $\vec{I}$ laser intensity. This system of partial differential equations is completed by the equation of state which gives pressure $p = p(\rho, e)$ and temperature $T = T(\rho, e)$ as functions of density and internal energy. Many simulated problems in laser plasma involve however complex flows with e.g. shear waves or physical instabilities which deform Lagrangian mesh moved by the flow so much that it becomes invalid (with non-convex or even inverted cells) and Lagrangian computation cannot continue. Arbitrary Lagrangian Eulerian (ALE) method [3] offers a possibility to avoid distortions of moving Lagrangian meshes. After several time steps of Lagrangian simulation or when the

mesh becomes distorted, the deformed mesh is smoothed out by rezoning, the conservative quantities are conservatively remapped from the deformed mesh to the smother one and Lagrangian computation can continue.

Preliminary results of laser interaction with flyer targets have been presented in [4, 5]. These results were obtained by 2D Cartesian ALE code with disc flyer impacting data estimated from 1D code modeling disc flyer acceleration. The ALE code have been extended by cylindrical geometry and here we present results in cylindrical geometry with disc flyer acceleration simulated in 2D.

2 Numerical ALE method with extensions

Our 2D ALE code [6] employs conservative, compatible Lagrangian hydrodynamical algorithm [7], classical Winslow mesh smoothing technique and efficient swept area remapping method [8] with subcell remapping of all conservative quantities [9]. For the Lagrangian step in cylindrical geometry we use a version of control volume method [7]. The smoothing remains in cylindrical geometry the same as in Cartesian one while the remapping has been generalized to cylindrical geometry [6]. As equation of state we apply quotidial equation of state QEOS [10] which approximates plasma behavior in reasonably large area of plasma parameters. The parabolic part of the energy equation dealing with heat conductivity is treated separately by splitting by numerical mimetic method [11] with classical Spitzer-Harm heat conductivity [12] and heat flux limitation by $Q_{lim} = fkn_e v_{Te} T_e$ where n_e is the electron density, k Boltzmann constant, v_{Te} thermal velocity of electrons, T_e electron temperature and we have used the limiter $f = 0.05$. The laser absorption in the energy equation is included in hyperbolic hydrodynamics part as a source term with laser being absorbed on the critical surface with estimated absorption coefficient.

3 Laser interactions with flyer targets

Using the developed ALE code we model flyer target experiments performed at the Prague Asterix Laser System (PALS) [1, 2]. The experimental setup of these experiments is shown in Fig. 1. The Aluminum disc flyer of thickness d and radius r is located in the distance L from the Aluminum massive target. The disc flyer is irradiated by intense laser pulse and ablatively accelerated towards massive target. The high velocity impact of the disc flyer on the massive target creates a crater in the massive target.

Particular geometrical data of the simulated experiments include: the disc radius $r = 150\,\mu$m, the disc thickness $d = 6\,\mu$m or $d = 11\,\mu$m and initial distance of the disc from target $L = 200\,\mu$m. The disc is irradiated by iodine laser pulse with energy $E = 120\,\mathrm{J}, 130\,\mathrm{J}, 240\,\mathrm{J}$ or $390\,\mathrm{J}$ on basic wave length $\lambda_1 = 1.315\,\mu$m and $E = 130\,\mathrm{J}$ on the third harmonics $\lambda_3 = 0.438\,\mu$m. The radius of laser spot on target is $r_f = 125\,\mu$m and the pulse duration (FWHM - full width half maximum) is 400 ps. Assumed temporal and spatial Gaussian laser profiles approximate experiment reasonably

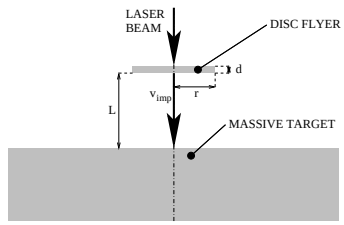

Fig. 1. Experimental setup.

well. We estimate the laser absorption to 50 % for the first harmonics and to 75 % for the third harmonics.

The simulation is split into two parts: ablative acceleration of disc flyer and high velocity impact of the disc flyer on the massive target. The result of the first part, the accelerated disc flyer for 6 μm thick disc with 130 J laser pulse on the third harmonics is shown in Fig. 2 presenting density and computational mesh at time $t_{\mathrm{imp}} = 0.7$ ns after the pulse maximum just before the disc flyer hits the massive target. The green line in Fig. 2 denotes the massive target surface and the red curve is zero contour of the vertical z velocity component, i.e. the disc material below this curve is flying down towards the massive target while the material above this curve is moving up. The mass weighted averaged values of density, temperature and velocity in higher density rectangular region for all simulated experiments at time of impact t_{imp} are summarized in Table 1 presenting also the measured experimental disc flyer velocities. The simulated disc flyer velocities are generally somewhat higher than experimental ones. For iodine laser basic frequency with 120 J energy a and for the third harmonic frequency the velocities are reasonably close. For the other two problems for which the experimental velocity is available the agreement with simulation velocity is not so good. The hydroefficiency, defined as the ratio of kinetic energy of disc material moving down towards the massive target to the total absorbed laser energy is in the range 5-12 % for the problems with laser on the first harmonics and 17 % for the problem with laser on the third harmonics.

The initial data for the second part of the simulation (high velocity impact) are obtained by conservative interpolation of the results of the first part (disc flyer acceleration) on the newly constructed mesh. The initial density for impact simulation presented in Fig. 3(a) has been obtained by interpolation of the acceleration results in Fig. 2. The pure Lagrangian codes are unable to simulate the high velocity impact problems as the moving mesh degenerates in the region around the disc edge rather soon. We demonstrate this behaviour in Fig. 3(b) presenting density of pure Lagrangian computation at time $t = 0.5$ ns. The computational mesh is already distorted rather seriously, soon after this time the mesh tangles and Lagrangian computation cannot continue as its assumptions are violated. The full

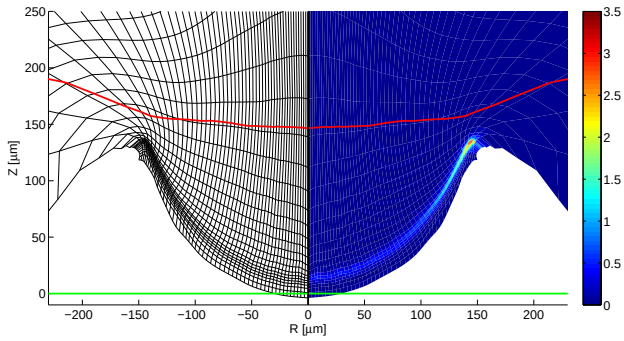

Fig. 2. Density (in g/cm^3) and computational mesh of 6 μm thick disc accelerated disc by laser pulse of energy 130 J at the third harmonic at time $t_{\mathrm{imp}} = 0.7$ ns.

Table 1. Average values in the higher density region of the impacting disc: time of impact t_{imp}, disc density ρ_{avg}, disc temperature T_{avg}, impact velocity v_{imp}, and experimental impact velocity v_{exp}. Symbol "?" denotes unavailable experimental velocity.

Problem	t_{imp}[ns]	ρ_{avg}[g/cm^3]	T_{avg}[eV]	v_{imp}[km/s]	v_{exp}[km/s]
6 μm, 130 J, 1st	1.8	0.07	7.7	88	60
6 μm, 130 J, 3rd	0.7	0.07	43.9	153	150
11 μm, 120 J, 1st	3.0	0.11	3.4	46	40
11 μm, 240 J, 1st	2.0	0.13	6.5	76	54
11 μm, 390 J, 1st	1.6	0.13	10.5	104	?

ALE method deals with problems with mesh distortion and produces reasonable results.

The disc flyer in plasma state hits the massive target in high velocity and starts to melt and evaporate target material creating the crater in the target. The impact creates approximately circular shock wave which propagates into the target and can be seen in Fig. 4 in solid material. The evaporated material moves in the direction opposite to impacting disc speed creating corona like shape. The results at time $t = 80$ ns after the impact are presented in Fig. 4 in the form of temperature with computational mesh (a) and internal energy increase (b). Different phases of Aluminum are shown in different colormaps, solid phase in shades of gray, liquid phase in rainbow colors and gas phase in shades of brown. The isolines distinguishing the phases in temperature are given by Aluminum melting and boiling points. The isolines distinguishing the phases in internal energy are given by specific heat needed to heat Aluminum to melting or boiling point together with heat of fusion and heat of vaporization needed for melting and evaporation of Aluminum. As the employed QEOS equation of state [10] does not include heat of fusion and heat of vaporization the temperature and internal energy plots give different phase interfaces. By crater we understand the liquid gas phase interface. The crater depth

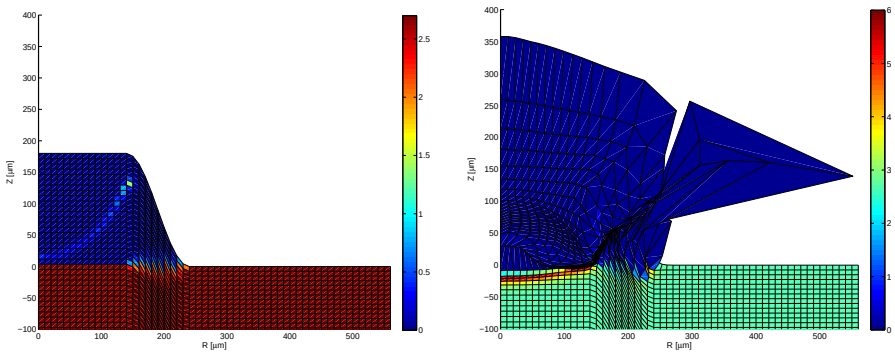

(a) initial data (b) pure Lagrangian at $t = 0.5\,\mathrm{ns}$

Fig. 3. Density (in g/cm^3) and computational mesh of 6 μm thick disc irradiated by 130 J laser beam on third harmonic. Data from Figure 2 interpolated to initial impact mesh (a) and density at time $t = 0.5\,\mathrm{ns}$ by purely Lagrangian computation (b).

and radius estimated from temperature and internal energy simulation results are compared with the experimental data for all investigated cases in Table 2. For lower energies 120 J and 130 J the estimates from temperature correspond better to the experimental crater sizes while for higher energies 240 J and 390 J the internal energy estimates are closer to the experimental measurement. The simulated results correspond to experimental measurements reasonably well.

For the disc acceleration simulation we have used 50×50 computational mesh with initially geometrically increasing or decreasing mesh steps with geometrical factors 1.02 in r direction and 0.95 in z direction. For the impact simulation we have used 150×200 mesh part of which is shown in Fig. 3(a). The heat conductivity effects are essential for the ablative acceleration of the disc while they influence the impact simulation only very little. The ALE method is essential for the impact simulation where we perform mesh smoothing/remapping after every ten Lagrangian time steps.

Table 2. Comparison of crater depth D_c and radius R_c (in μm) according to temperature and specific internal energy increase.

Problem	experiment		temperature		energy	
	D_c	R_c	D_c	R_c	D_c	R_c
6 μm, 130 J, 1st	300	300	350	290	210	260
6 μm, 130 J, 3rd	550	500	470	470	320	420
11 μm, 120 J, 1st	280	300	270	280	200	260
11 μm, 240 J, 1st	320	320	460	330	300	310
11 μm, 390 J, 1st	380	400	530	370	450	340

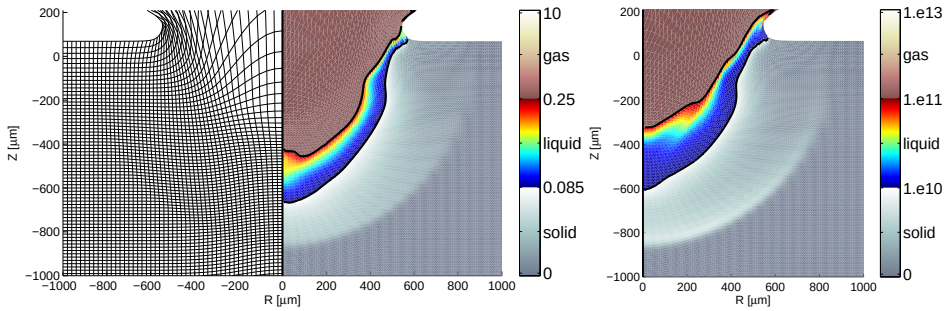

(a) computational mesh and temperature (b) internal energy increase

Fig. 4. Computational mesh (only every second edge in each logical direction is visible) and temperature (in eV) (a) and specific internal energy increase (in erg/g) (b) of 6 μm thick disc irradiated by 130 J laser beam on third harmonic at time $t = 80$ ns after the impact. Solid, liquid and gas phases are separated by isolines in temperature and energy increase of melting and evaporation of Aluminum, different material phases are shown in different colormaps.

This research has been partly supported by the Czech Ministry of Education project MSM 6840770022, research center LC 528 and the Czech Science Foundation project GACR 202/03/H162. The authors thank R. Garimella, P. Havlík, R. Loubère, M. Shashkov and B. Wendroff for fruitful discussions and constructive comments.

References

[1] M. Kalal et.al: *Proceedings of 28th ECLIM* (2005) 249–259.

[2] S. Yu. Guskov and et.al. *J. of Russian Laser Research* **26** (2005) 228–244.

[3] C. W. Hirt, A. A. Amsden, J. L. Cook: *J. Comp. Phys.* **14** (1974) 227–253. Reprinted at *J. Comp. Phys.* **135** (1997) 203–216.

[4] M. Kuchařík et.al: *Czechoslovak Journal of Physics* **54** (2004) C391–C396.

[5] M. Kuchařík et.al:*Proceedings of 28th ECLIM* (2005) 470–474.

[6] M. Kuchařík: PhD thesis (2006). Czech Technical University in Prague.

[7] E. J. Caramana et.al:*J. Comp. Phys.* **146** (1998) 227–262.

[8] M. Kuchařík, M. Shashkov, B. Wendroff: *J. Comp. Phys.* **188** (2003) 462–471.

[9] R. Loubere, M. Shashkov: *J. Comp. Phys.* **209** (2005) 105–138.

[10] R. M. More, K. Warren, D. Young, G. Zimmerman: *Phys. Fluids* **31** (1988) 3059–3078.

[11] M. Shashkov, S. Steinberg: *J. Comp. Phys.* **129** (1996) 383–405.

[12] L. Spitzer, R. Harm. *Phys. Rev.* **89** (1953) 977–981.